Available online at www.sciencedirect.com
ScienceDirect
Journal of the European Ceramic Society 29 (2009) 3219–3225
www.elsevier.com/locate/jeurceramsoc

Thermal expansion of zirconia–zirconium titanate materials obtained by slip casting of mixtures of Y-TZP–TiO_2

Emilio López-López, Carmen Baudín, Rodrigo Moreno *

Instituto de Cerámica y Vidrio (CSIC), C/ Kelsen 5, 28049 Madrid, Spain

Received 3 April 2009; received in revised form 28 May 2009; accepted 10 June 2009
Available online 14 July 2009

Abstract

The objective of this work was to establish the optimum conditions to get zirconia materials with different proportions of zirconium titanate by reaction sintering of ZrO_2 stabilized with 3 mol% of Y_2O_3 (Y-TZP) and TiO_2. The green bodies were fabricated from stable colloidal suspensions of the powders by slip casting in plaster moulds.

The rheological characterization of the suspensions allowed the establishment of the optimum green processing conditions. Reaction sintering was performed at 1500 °C during 2 h, and the obtained materials have been characterized by X-ray diffraction (XRD) and field emission scanning electron microscopy with energy dispersive X-ray microanalysis (FE-SEM-EDX). Under these conditions, zirconium titanate materials with tetragonal zirconia could not be obtained because a solid solution of cubic zirconia with titania and yttria is formed at 1500 °C. The thermal expansion of the materials was determined by differential dilatometry from room temperature up to 850 °C, demonstrating that the incorporation of zirconium titanate reduces the thermal expansion of zirconia.

Keywords: Suspensions; Sintering; ZrO_2; Zirconium titanate; Thermal expansion

1. Introduction

Zirconium titanate materials are well known for electroceramics applications,[1–3] due to their good thermal and electrical properties. Nevertheless, this kind of materials has not been usually considered for structural applications although the stoichiometric zirconium titanate, $ZrTiO_4$, presents crystallographic anisotropy in thermal expansion ($\alpha_{a25–800\,°C} = 6.2 \times 10^{-6}\,°C^{-1}$, $\alpha_{b25–800\,°C} = 10 \times 10^{-6}\,°C^{-1}$, $\alpha_{c25–800\,°C} = 8.6 \times 10^{-6}\,°C^{-1}$ [4]),[a] so that it could be successfully used as constituent of low thermal expansion materials.

Synthesis of zirconium titanate can be made by different methods like co-precipitation,[5,6] sol–gel,[7–11] mechanochemical processing[12] and solid-state reaction from ZrO_2 and TiO_2 powders.[13] A suitable method to get zirconia-based materials with zirconium titanate as second phase is the reaction sintering of pieces obtained by slip casting of concentrated slurries of ZrO_2 and TiO_2.[14,15] This method enables manufacturing a wide range of zirconia materials, with different relative contents of zirconium titanate.

The rheological characterization of the starting slurries is a key tool to determine the optimal dispersing conditions to prepare stable concentrated suspensions to be successfully slip cast in plaster moulds and to obtain defect-free green materials with high relative density. The optimal conditions to obtain well-dispersed slurries of zirconia and titania were established in a previous work.[14]

The aim of this work was to synthesize zirconia/zirconium titanate composites with different relative concentrations of zirconium titanate by reaction sintering of green bodies obtained by slip casting suspensions of ZrO_2 stabilized with 3 mol% of Y_2O_3 and TiO_2, and to determine the thermal expansion behaviour of the resulting sintered materials, as a basic parameter for structural applications.

2. Experimental

Commercial ZrO_2 stabilized with 3 mol% of Y_2O_3 (yttria-tetragonal zirconia polycrystal Y-TZP, TZ3YS, TOSOH, Tokyo,

* Corresponding author. Tel.: +34 917355840; fax: +34 917355843.
E-mail address: rmoreno@icv.csic.es (R. Moreno).

[a] Lattice: orthorhombic; space group: *Pnab*; $a = 5.03580$ nm, $b = 5.48740$ nm, and $c = 4.80180$ nm. ASTM 34-415.

0955-2219/$ – see front matter © 2009 Elsevier Ltd. All rights reserved.
doi:10.1016/j.jeurceramsoc.2009.06.003

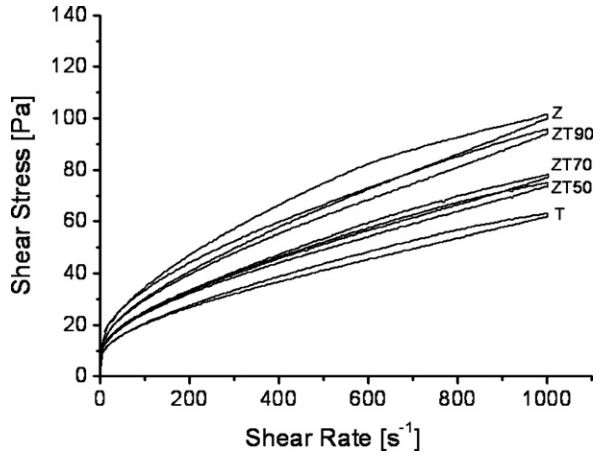

Fig. 1. Flow curves of Z, ZT90, ZT70, ZT50 and T suspensions.

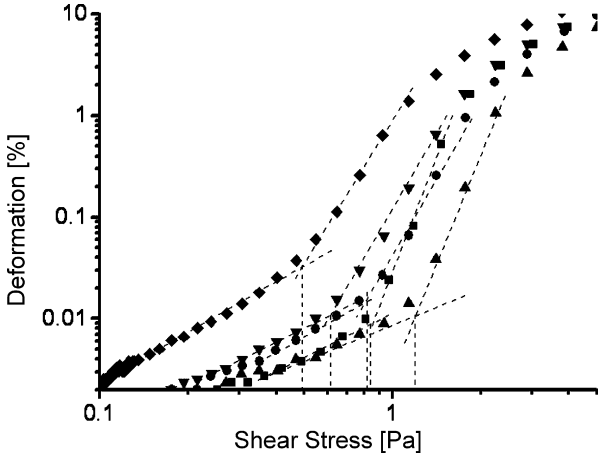

Fig. 2. Log/log deformation versus stress curves of Z (▲), ZT90 (■), ZT70 (●), ZT50 (▼) and T (♦) slurries. The intersection points between the two linear regions indicate the yield points of the different slurries, reported in Table 1.

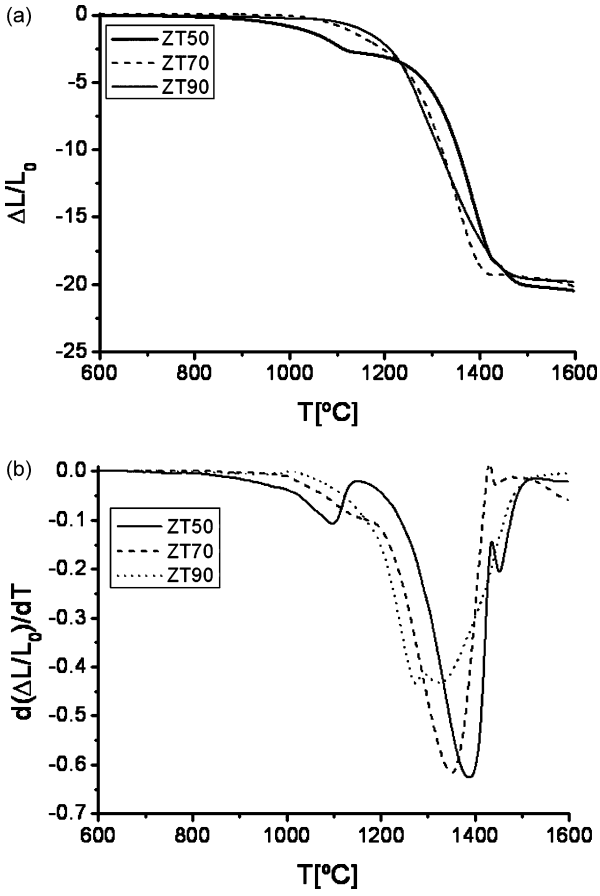

Fig. 3. (a) Shrinkage versus temperature recorded during the heating part of the cycle and (b) derivative versus temperature of the curves plotted in Fig. 3a.

Japan) and anatase-TiO_2 (Merck, 808, Darmstadt, Germany) were used as precursor powders. These powders have average particle diameters of 0.4 and 0.3 μm, respectively, and specific surface areas of 6.7 and 9.0 m^2/g, respectively.

The particle size distribution was determined with a laser diffraction analyser (Mastersizer S, Malvern, Worcestershire, United Kingdom), and the specific surface area was measured by the N_2 adsorption method (Monosorb Surface Area Analyser MS13, Quantachrome Co., FL, USA).

Concentrated suspensions of Y-TZP (Z) and TiO_2 (T) were prepared separately to 45 vol.% solids (83 and 76 wt.%, respectively) by adding the powder to the proper amount of deionised water containing polyacrylic-based dispersant (Dolapix CE64, Zschimmer-Schwarz, Lahnstein, Germany) to a total concentration of 0.8 wt.% on a dry solids basis, and further mixing with a high shear mixer (Silverson, L2R, Chesham, United Kingdom). Then, they were ball milled for 24 h using alumina jar and balls. The as-prepared one component suspensions were mixed to relative molar ratios of 90:10, 70:30 and 50:50 in order to obtain ZT90, ZT70 and ZT50 suspensions, respectively. The resulting mixtures were then ball milled for 1 h to assure uniform mixing. Details of the preparation procedure are given in a previous work.[14]

For the rheological characterization of the suspensions a rotational rheometer (Thermo-Haake, RS50 Thermo, Karlsruhe, Germany) with a double cone/plate geometry was used. Flow

Table 1
Rheological parameters of suspensions and density of green casts.

Suspension	Viscosity at 500 s^{-1} (mPa s)	Tixotropy (Pa/s)	Yield point (Pa)	Green density (g/cm^3)	Relative density (%)
Z	148 ± 5	5200 ± 600	1.2	3.2 ± 0.1	54 ± 1
ZT90	128 ± 10	2600 ± 1000	0.8	3.1 ± 0.1	54 ± 1
ZT70	106 ± 1	2500 ± 200	0.8	3.0 ± 0.1	56 ± 1
ZT50	105 ± 1	1800 ± 400	0.6	3.0 ± 0.1	60 ± 1
T	87 ± 7	1950 ± 300	0.5	2.2 ± 0.1	56 ± 1

Table 2
Density of materials sintered at 1500 °C/2 h and average thermal expansion coefficient between 25 and 850 °C.

Material	Sintered density (g/cm^3)	$\alpha_{25-850} \times 10^{-6}$ (°C^{-1})
Z1500	6.1 ± 0.1	10.6 ± 0.2
ZT901500	5.9 ± 0.1	10.4 ± 0.5
ZT701500	5.5 ± 0.1	8.7 ± 0.3
ZT501500	5.0 ± 0.1	6.7 ± 0.2

curves were performed by changing shear rate between 0 and 1000 s^{-1} for 5 min, for both the up and the down ramps with a 1 min stay at the maximum rate. Temperature was maintained constant at 25 °C. All suspensions were prepared and measured at least three times and representative curves are given. Measurements were also performed under controlled stress mode (CS), where the applied shear stress increases from 0 to 1 Pa in 3 min, and comes back to 0 in the same time. Yield points were calculated from the log/log plots of shear stress versus deformation measured in CS mode. These plots yield two straight lines which intersection is considered as the yield stress value.

The green bodies were shaped into plates of 70 mm × 70 mm × 10 mm by slip casting the ZT90, ZT70 and ZT50 suspensions in plaster moulds and dried in air for 48 h. Specimens for the different tests were obtained by cutting these plates.

Green and sintered densities were determined by the Archimedes' method, using mercury and deionised water, respectively. Relative densities of green samples (% of theoretical) were calculated taking into account that the starting Y-TZP contained 70 wt.% of tetragonal phase (density = 6.07 g/cm^3, ASTM 83-113) and 30 wt.% of monoclinic phase (density = 5.82 g/cm^3, ASTM 37-1484), as determined by

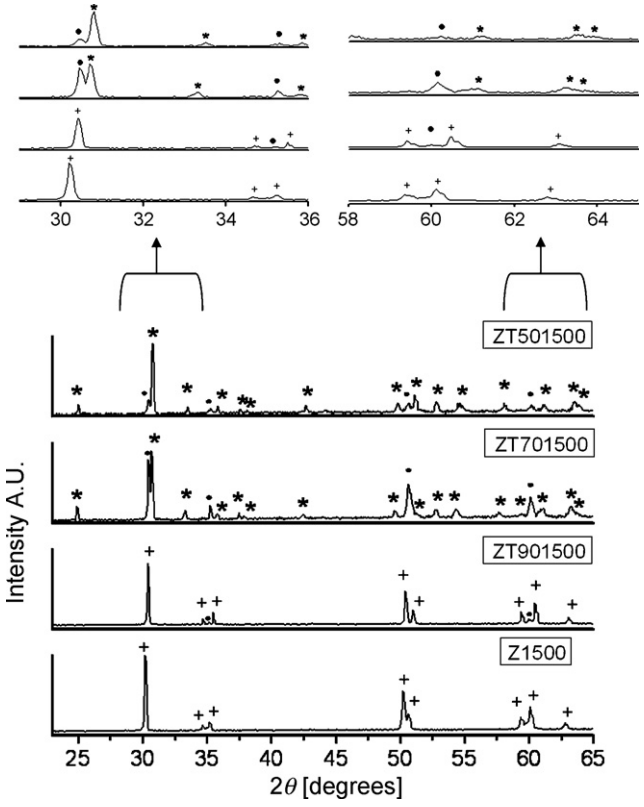

Fig. 4. XRD spectra of Z15002h, ZT9015002h, ZT7015002h and ZT5015002h materials. (*) $Zr_5Ti_7O_{24}$, (●) c-ZrO_2ss, and (+) t-ZrO_2ss.

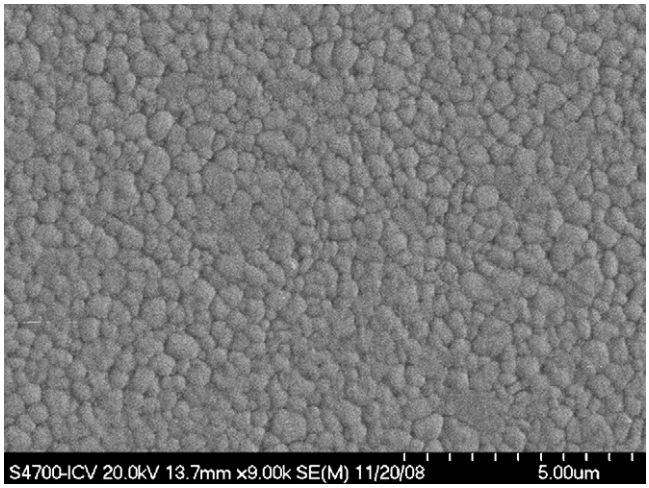

Fig. 5. Microstructure of Z15002h material. FE-SEM micrograph of polished and thermally etched (1400 °C/1 min) surface.

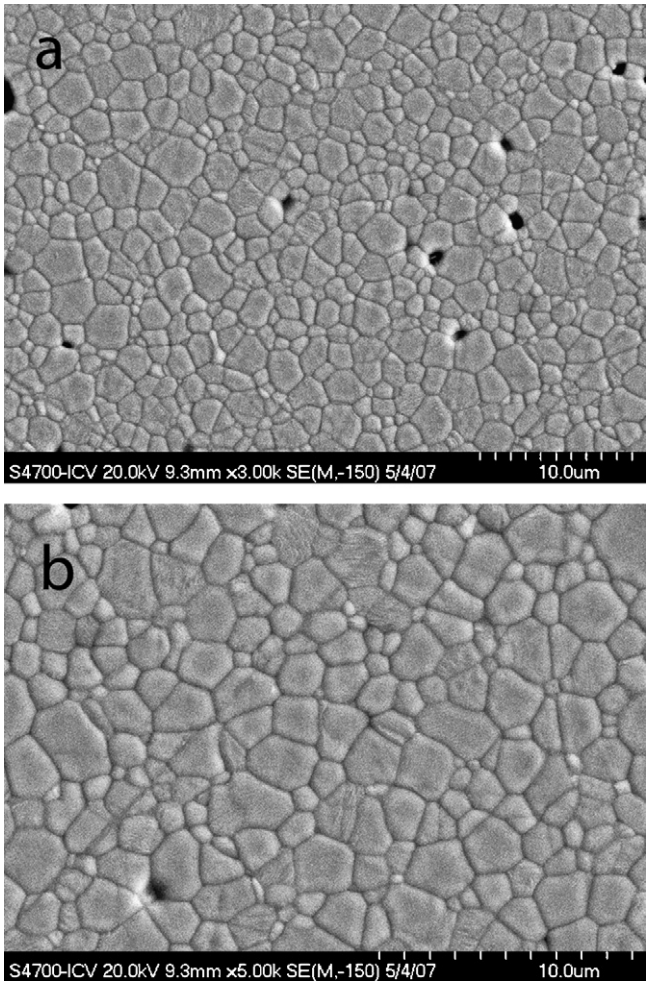

Fig. 6. Microstructure of ZT9015002h material. FE-SEM micrographs of polished and thermally etched (1400 °C/1 min) surfaces.

X-ray diffraction of the powders, the resulting density being 6.00 g/cm^3, and using 3.89 g/cm^3 as density for anatase-TiO_2 (ASTM 21-1272).

Constant heating rate (CHR, heating and cooling rates 5 °C/min) experiments up to 1600 °C were performed in a differential dilatometer with alumina rod (Adamel Lhomargy, DI24, Brie France). From the results of the dilatometric analyses of ZT90, ZT70 and ZT50, the heating temperature selected to sinter the different materials was 1500 °C for 2 h, with heating and cooling rates of 5 °C/min, and were named Z1500, ZT901500, ZT701500 and ZT501500.

Phase analysis was done by X-ray diffraction (XRD) in bulk pieces using a Siemens D5000 diffractometer (Munich, Germany). The obtained XRD patterns were analysed using the diffraction files of $Zr_5Ti_7O_{24}$ (ASTM 34-209), $Zr_{0.963}Y_{0.037}O_{1.982}$ (ASTM 83-113), and $Zr_{0.62}Y_{0.20}Ti_{0.18}O_{1.90}$.[16]

The microstructures of diamond polished (down to 3 μm) samples were characterized by field emission scanning electron microscopy with energy dispersive X-ray microanalysis (FE-SEM-EDX, Hitachi S-4700 type I, Tokyo, Japan).

Pieces of 10 mm × 10 mm × 5 mm cut from the sintered blocks were tested in a differential dilatometer (402 EP, Netzsch, Germany) to obtain the thermal expansion curves from tests with heating and cooling rates of 2 °C/min. Three determinations were performed for each material. Results for the average thermal expansion coefficients are the average of the three determinations and errors are the standard deviations.

3. Results and discussion

3.1. Rheological characterization

Fig. 1 shows the flow curves obtained from the control rate measurements of the different suspensions prepared to 45 vol.% solids. From this figure it can be observed that the increase of TiO_2 concentration in the suspensions improves the rheological behaviour of the slurries, decreasing both the viscosity and the thixotropy. This can be observed better in Table 1, which summarises the rheological parameters of the slurries such as the values of viscosity at a shear rate of 500 s^{-1}, the calculated thixotropy and the yield stress values. Thixotropy values were calculated as the area enclosed between the up and down curves in the CR flow curves. Deviations of viscosity and thixotropy given in Table 1 are the experimental variations obtained for three different suspensions prepared and measured independently.

Fig. 2 shows the controlled stress measurements obtained from double logarithmic plot of deformation versus shear stress. These values are also given in Table 1, and show that increasing

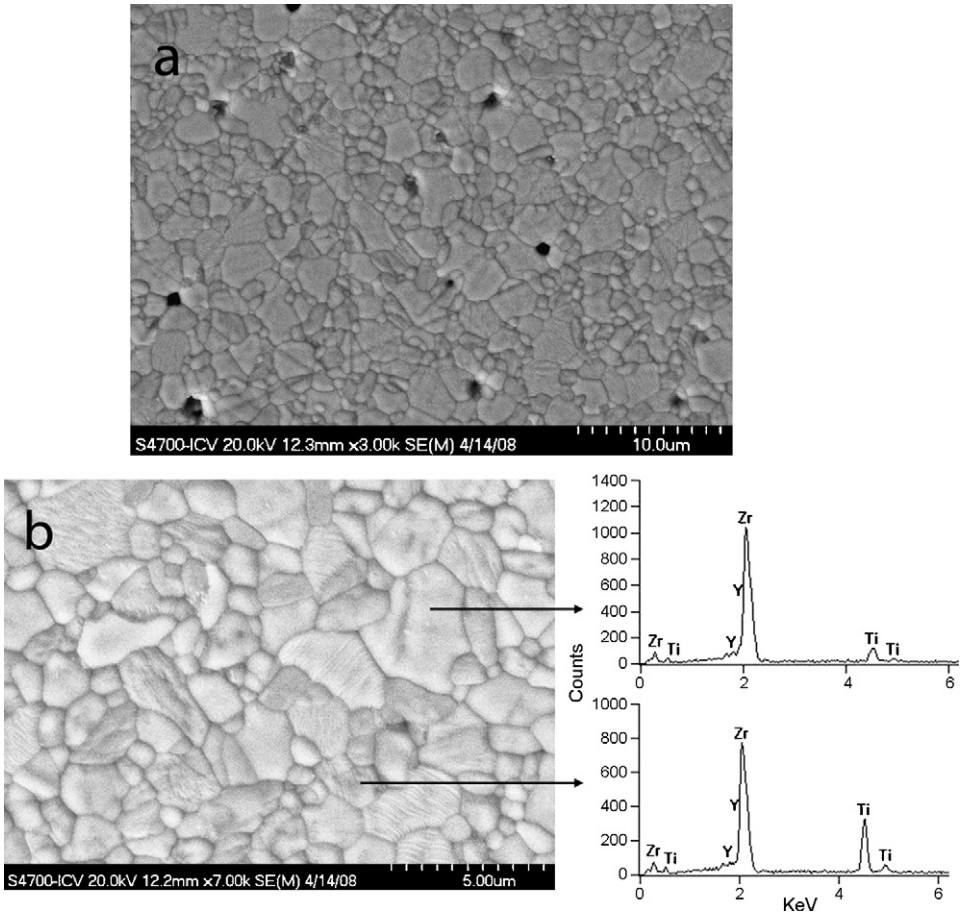

Fig. 7. Microstructure of ZT7015002h material. FE-SEM micrographs of polished and thermally etched (1400 °C/1 min) surfaces, together with characteristic EDX analyses.

amounts of TiO_2 in the suspension decrease their yield points, so that shear flow occurs very easily.

The green densities of the compacts obtained by slip casting of the suspensions are reported in Table 1. It can be seen that the relative density values were higher for T than for Z, and in the mixtures it increases with relative T contents probably because the viscosity and yield points of the starting suspensions were lower.

3.2. Reaction sintering process

Details of reaction sintering process of the material ZT50 were studied in a previous work[15] and have been used as a reference. In this work the sintering behaviour of the different compositions is studied and compared with the ZT50 reference material.

Results from CHR experiments are plotted in Fig. 3. It can be observed that even though increasing amounts of TiO_2 decreased the temperature of initial shrinkage, they increased the temperature of maximum shrinkage rate. Shrinkage of both compacts ZT70 and ZT50 was arrested at temperature ≈1440 °C, above the maximum densification rate (≈1350 and ≈1390 °C, respectively), indicating the formation of zirconium titanate.[15] On the contrary, no feature in the derivative curve of ZT90 could be associated to the formation of zirconium titanate. In this case, the whole 10 mol% of TiO_2 might incorporate inside the ZrO_2 lattice as a solid solution, as reported by other authors,[16–20] impeding zirconium titanate formation, at least at significant amounts to be detected by XRD.

From the above discussion, the selected temperature for the fabrication of the materials to guarantee the formation of zirconium titanate was 1500 °C and hence further experiments were performed for this sintering temperature.

3.3. Materials characterization

Selected properties of the sintered materials Z1500, ZT901500, ZT701500 and ZT501500 are summarised in Table 2.

Fig. 4 shows the XRD patterns of the sintered compacts. As expected, the reference Z1500 material was only formed by t-ZrO_2, and it had a homogeneous microstructure with small grain size (Fig. 5).

In agreement with the CHR results above discussed, zirconium titanate was not detected in ZT901500; ZrO_2 in this material was present as t-ZrO_2ss (major phase) and as c-ZrO_2ss (second phase). Fig. 6 shows the microstructure of a ZT901500 specimen, where the coarsest grains correspond to c-ZrO_2ss.

The XRD pattern of ZT701500 (Fig. 4) shows that it was formed by the low-temperature phase of zirconium titanate ($Zr_5Ti_7O_{24}$) and c-ZrO_2ss. This latter phase is the one reported by Feighery et al.,[16] with large amounts of Y_2O_3 (18.0 wt.%) and TiO_2 (11.4 wt.%) in solid solution. Both phases can be differentiated in the micrographs of this material (Fig. 7). The corresponding EDX analysis of the different sized grains confirms that the smallest grains were $Zr_5Ti_7O_{24}$ and the biggest corresponded to c-ZrO_2ss.

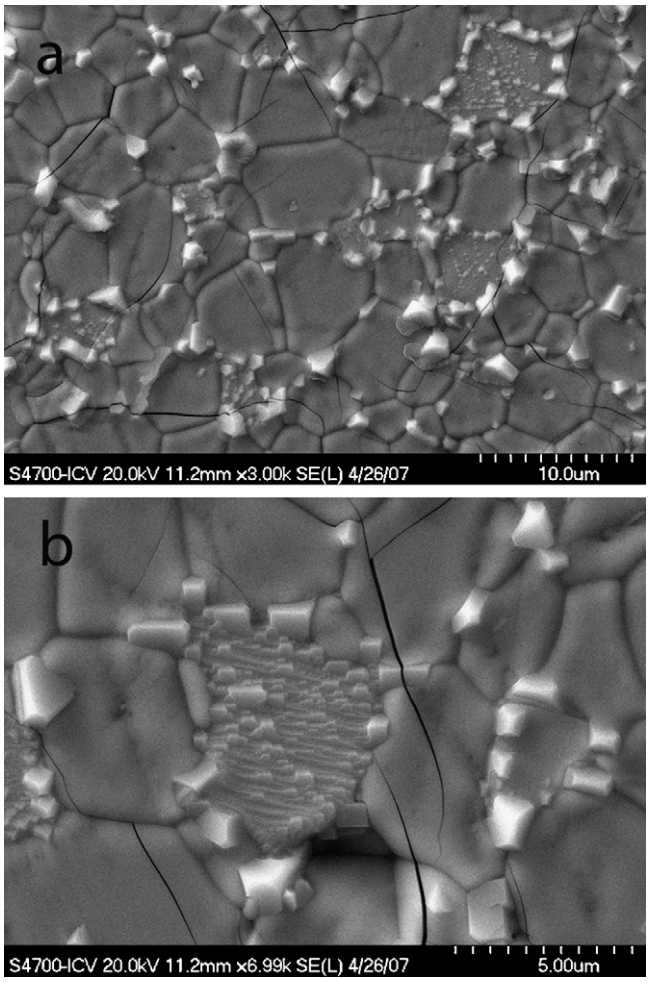

Fig. 8. Microstructure of ZT5015002h material. FE-SEM micrographs of polished and thermally etched (1400 °C/1 min) surfaces.

Fig. 8 shows the microstructure of the ZT501500 material. Although its XRD pattern (Fig. 4) corresponds to a biphasic material, the in-depth analysis of the different types of grains performed by EDX (Fig. 8) demonstrates that it was formed by three phases, $Zr_5Ti_7O_{24}$, c-ZrO_2ss and pyrochlore-type phase ($Y_2Ti_{2-x}Zr_xO_7$), where the c-ZrO_2 presented the same structure as that observed in ZT701500. Details of the microstructure of this material were studied in a previous work.[15]

It is important to remark that in these materials the low-temperature phase of zirconium titanate was present due to the presence of Y_2O_3 that promotes zirconium titanate transformation on cooling.[21–23]

The thermal expansion curves of the studied materials are plotted in Fig. 9 and values of the average thermal expansion coefficients between room temperature and 850 °C are summarised in Table 2. It can be observed that materials without $Zr_5Ti_7O_{24}$, Z1500 and ZT901500, presented similar thermal expansion behaviours, while the incorporation of zirconium titanate, ZT701500 and ZT501500, clearly reduces the thermal expansion coefficient. The presence of microcracks in ZT501500 (Fig. 8) also helps to reduce the thermal expansion of this material, but they did not lead to a widespread crack-

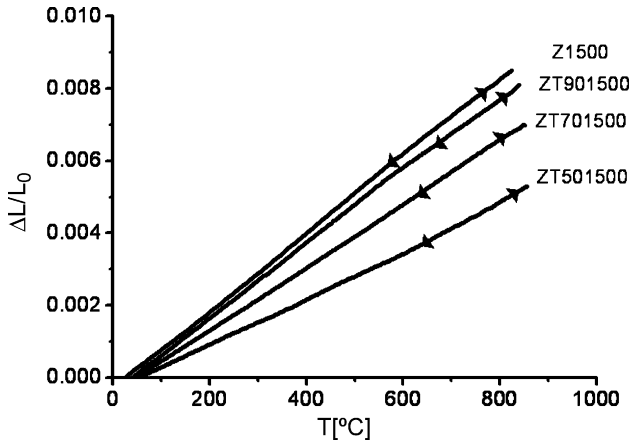

Fig. 9. Thermal expansion curves of Z15002h, ZT9015002h, ZT7015002h and ZT5015002h materials on heating and cooling at 2 °C/min. Heat and cooling curves coincide with the curve width. Z1500 curve has been displaced 25 units towards the left to avoid matching up with ZT901500 curve.

ing of the material. Therefore, the absence of microcracks in Z1500, ZT901500 and ZT701500 materials, their shorter length in the ZT501500 one explains the lack of hysteresis in their corresponding thermal expansion curves.

Thus, it has been demonstrated that zirconium titanate is a good candidate for manufacturing zirconia ceramics with low thermal expansion. Further studies should be directed towards the enhancement of t-ZrO_2 formation at the expense of c-ZrO_2. Even though there is not a general agreement about the phase equilibrium relationships in the ZrO_2–Y_2O_3–TiO_2 system, reported data indicate that to enhance t-ZrO_2 formation in compositions treated at 1500 °C, the amounts of Y_2O_3 should be decreased.[20]

4. Conclusions

The rheological behaviour of suspensions of ZrO_2 stabilized with 3 mol% of Y_2O_3 and TiO_2 has been optimised before mixing them in the required quantities to obtain green compacts with 90, 70 and 50 mol% of Y-TZP.

The best homogenization was achieved by mixing both monophasic suspensions by ball milling for 1 h. Solids loading was always 45 vol.%. The pure Z suspension has the highest viscosity and thixotropy and rheological parameters decrease as the TiO_2 content increases. Slip cast bodies were treated at 1500 °C/2 h to promote the formation of zirconium titanate by reaction sintering. Materials with 10 mol% of TiO_2 did not form the zirconium titanate phase, because TiO_2 forms solid solutions with t-ZrO_2 and c-ZrO_2.

Materials with different contents of zirconium titanate and c-ZrO_2ss either as main phase or second phase are formed, but it was not possible to obtain materials of zirconium titanate with tetragonal zirconia under the studied conditions. This is attributed to the presence of Y_2O_3 that promotes the formation of the low-temperature phase of zirconium titanate and favours the formation of the cubic phase of zirconia.

The results shown herein demonstrate that the incorporation of zirconium titanate reduces the thermal expansion of zirconia materials, and therefore, it can be used to obtain low thermal expansion materials.

Acknowledgements

This work has been supported by MICINN under contract MAT2006-13480 C02-01. López-López acknowledges Comunidad de Madrid (Spain) and European Social Fund for economical support by CPI/0552/2007 contract.

References

1. Wang, C. L., Lee, H. Y., Azough, F. and Freer, R., The microstructure and microwave dielectric properties of zirconium titanate ceramics in the solid solution system $ZrTiO_4$–$Zr_5Ti_7O_{24}$. *J. Mater. Sci.*, 1997, **32**, 1693–1701.
2. Wakino, K., Minai, K. and Tamura, H., Microwave characteristics of (Zr,Sn)TiO_4 and BaO–PbO–Nd_2O_3–TiO_2 dielectric resonators. *J. Am. Ceram. Soc.*, 1984, **67**, 278–281.
3. Leoni, M., Viviani, M., Battilana, G., Fiorello, A. M. and Viticoli, M., Aqueous synthesis and sintering of zirconium titanate powders for microwave components. *J. Eur. Ceram. Soc.*, 2001, **21**, 1739–1741.
4. Ikawa, H., Iwai, A., Iruta, K., Shimojima, H., Urabe, K. and Udagawa, S., Phase transformation and thermal expansion of zirconium and hafnium titanates and their solid solutions. *J. Am. Ceram. Soc.*, 1988, **71**, 120–127.
5. Kudesia, R., Snyder, R. L., Condrate, R. D and McHale Sr., A. E., Structural study of $Zr_{0.8}Sn_{0.2}$ TiO_4. *J. Phys. Chem. Solids*, 1993, **54**, 671–684.
6. Krebs, M. A. and Condrate Sr., R. A., A Raman spectral characterization of various crystalline mixtures in the ZrO_2–TiO_2 and HfO_2–TiO_2 systems. *J. Mater. Sci. Lett.*, 1988, **7**, 1327–1330.
7. Bhattacharya, A. K., Mallick, K. K., Hartridge, A. and Woodhead, J. L., Sol gel preparation, structure and thermal stability of crystalline zirconium titanate microspheres. *J. Mater. Sci.*, 1996, **31**, 267–271.
8. Navío, J. A., Marchena, F. J., Macias, M., Sanchez-Soto, P. J. and Pichat, P., Formation of zirconium titanate powder from a sol–gel prepared reactive precursor. *J. Mater. Sci.*, 1992, **27**, 2463–2467.
9. Sahm, E. L., Aranda, M. A. G., Farfan-Torres, E. M., Gottifredi, J. C., Martinez-Lara, M. and Bruque, S., Zirconium titanate from sol–gel synthesis: thermal decomposition and quantitative phase analysis. *J. Solid State Chem.*, 1998, **139**, 225–232.
10. Hirano, S., Hayashi, T. and Hattori, A., Chemical-processing and microwave characteristics of (Zr,Sn)TiO_4 microwave dielectrics. *J. Am. Ceram. Soc.*, 1991, **74**, 1320–1324.
11. Cerqueira, M., Nasar, R. S., Longo, E., Leite, E. R. and Varela, J. A., Synthesis of ultrafine crystalline $Zr_xTi_{1-x}O_4$ powder by polymeric precursor method. *Mater. Lett.*, 1995, **22**, 181–215.
12. Gajovic, A., Furic, K., Music, S., Djerdj, I., Tonejc, A. and Tonejc, A. M., Mechanism of $ZrTiO_4$ synthesis by mechanochemical processing of TiO_2 and ZrO_2. *J. Am. Ceram. Soc.*, 2006, **89**, 2196–2205.
13. Ananta, S., Tipakontitikul, R. and Tunkasiri, T., Synthesis, formation and characterization of zirconium titanate (ZT) powders. *Mater. Lett.*, 2003, **57**, 2637–2642.
14. López-López, E., Baudín, C. and Moreno, R., Synthesis of zirconium titanate based materials by colloidal filtration and reaction sintering. *Int. J. Appl. Ceram. Technol.*, 2008, **5**, 394–400.
15. López-López, E., Sanjuan, M. L., Moreno, R. and Baudín, C., Phase evolution in reaction sintered zirconium titanate based materials, *J. Eur. Ceram. Soc.*, under review.
16. Feighery, A. J., Irvine, J. T. S., Fagg, D. P. and Kaiser, A., Phase relations at 1500 °C in the ternary system ZrO_2–Y_2O_3–TiO_2. *J. Solid State Chem.*, 1999, **143**, 273–276.
17. Noguchi, T. and Mizuno, M., Phase changes in the ZrO_2–TiO_2 system. *Bull. Chem. Soc. Jpn.*, 1968, **41**, 2895–2899.
18. Bannister, M. J. and Barnes, J. M., Solubility of TiO_2 in ZrO_2. *J. Am. Ceram. Soc.*, 1986, **69**, C269–C271.
19. Colomer, M. T., Durán, P., Caballero, A. and Jurado, J. R., Microstructure, electrical properties and phase equilibria relationships in the

ZrO_2–Y_2O_3–TiO_2 system: the subsolidus isothermal section at 1500 °C. *Mater. Sci. Eng. A*, 1997, **229**, 114–122.

20. Schaedler, T. A., Fabrichnaya, O. and Levi, C. G., Phase equilibria in the TiO_2–$YO_{1.5}$–ZrO_2 system. *J. Eur. Ceram. Soc.*, 2008, **28**, 2509–2520.
21. Bordet, P., McHale, A., Santoro, A. and Roth, R. S., Powder neutron diffraction study of $ZrTiO_4$, $Zr_5Ti_7O_{24}$, and $FeNb_2O_6$. *J. Solid State Chem.*, 1986, **64**, 30–46.
22. Azough, F., Freer, R. and Petzelt, J., A Raman spectral characterization of ceramics in the system ZrO_2–TiO_2. *J. Mater. Sci.*, 1993, **28**, 2273–2276.
23. Azough, F., Wright, A. and Freer, R., The microstructure and dielectric properties of $Zr_5Ti_7O_{24}$ ceramics. *J. Solid State Chem.*, 1994, **108**, 284–290.